

4. CHARACTERISTICS OF AN AGGREGATE OF ULTRAWIDEBAND SIGNALS

Roger A. Dalke¹

4.1 Introduction

The proliferation of UWB devices throughout the United States has been predicted by many industry sources. Hence, it is important that the effects of an aggregate of such devices on RF spectrum users be well understood by regulators, spectrum users, and UWB system designers. This section describes models that can be used to predict interference effects of many UWB devices on traditional narrowband RF receivers.

This model assumes that the *victim receiver* is *narrowband* and hence, it is sufficient to evaluate UWB parameters such as effective isotropically radiated average power (EIRP) and antenna gains at the center frequency of the receiver. The calculation of the power at the victim receiver requires an estimation of the basic transmission loss over the propagation path from the transmitters to the receiver. Single frequency propagation models used in traditional radio link calculations will be utilized in conjunction with the models described in this section. In the analysis which follows, it was convenient to use the basic transmission gain (denoted below as g_b) instead of loss. The basic transmission gain and loss are reciprocals and have the same absolute value but opposite signs when given in decibels.

In the first part of this section, the aggregate effects of a few similar devices in the immediate vicinity of a victim receiver are discussed. This is followed by the development of a statistical model that can be used to calculate the average received power from many UWB devices randomly distributed over the surface of the Earth. This model can be used to predict interference power for both terrestrial and airborne receivers.

4.2 Deterministic Interference Model for UWB Devices in the Vicinity of a Victim Receiver

The mean power in the receiver bandwidth due to UWB devices is simply the sum of the power received from each source or

$$w_r = \sum_{n=1}^N w_{t_n} g_{t_n} g_{b_n} g_{r_n} \quad , \quad (4.1)$$

¹The author is with the Institute for Telecommunication Sciences, National Telecommunications and Information Administration, U.S. Department of Commerce, Boulder, CO 80305.

where w_r is the received power, w_t is the emitted EIRP in the receiver bandwidth, g_t is the transmitter gain, and g_r is the receiver gain in the direction of the n^{th} transmitting device. When the locations of the devices are known and N is small, computing the received power is a relatively straightforward matter.

More realistically, one may have only a rough estimate of the ostensible number of such devices deployed in a particular geographic area (e.g., an average areal density) surrounding a particular RF receiver. In such cases, Equation 4.1 is not very useful since the parameters (perhaps the most important one being g_{b_n}) are not known. Hence statistical models and estimates are required to make any progress in predicting the potential for interference. The development of such a model is given in the next section.

Equation 4.1 is valid for commonly encountered random RF signals because the variance of the sum of zero mean random variables is the sum of the individual variances. When the received signals are normally distributed, the mean power is all that is needed to describe the statistics of the resulting interference. If there are many such devices with the same statistical properties (not necessarily normally distributed) then the statistics of the sum will approach a normal distribution [1]. In such cases, the models that predict the mean interference power provide the only statistic necessary to describe the process.

This leads directly to the question of how many signals must be added before the aggregate signal realistically appears to be normally distributed. Perhaps some insight can be gained by examining the results for a band limited fixed time-base dithered UWB signal as described in Section 3.3. In this example, the signal statistics are approximately normal for bandwidths well below the PRR. As the bandwidth increases, the absolute value of the excess increases and the statistics are no longer normal. The excess for an aggregate of such devices can be calculated as described below.

The aggregate excess for the sum of several random variables is related to the excess of each random variable γ_{2_n} as follows

$$\gamma_2 = \frac{\sum_n \gamma_{2_n} [\mu_{2_n}]^2}{\mu_2^2} \quad , \quad (4.2)$$

where μ_{2_n} is the second central moment of each variable and μ_2 is the sum of the moments. Since the processes are zero mean, the second central moment is just the signal power given in Equation 4.1.

The aggregate excess for band limited signals (e.g., as given in Section 3.3) is therefore

$$\gamma_2 = \frac{\sum_n \gamma_{2n} [w_{t_n} g_{t_n} g_{r_n} g_{b_n}]^2}{\left[\sum_n w_{t_n} g_{t_n} g_{r_n} g_{b_n} \right]^2} \quad (4.3)$$

When the individual excesses, EIRP, and gains are the same, Equation 4.3 reduces to the *well known* result

$$\gamma_2 = \frac{\gamma_{2n}}{N} \quad , \quad (4.4)$$

which indicates that the excess can decrease fairly rapidly as additional devices are added.

4.3 Statistical Aggregate Model

In this subsection, we develop a statistical model that can be used to estimate received interference power from many devices randomly distributed over the area surrounding a victim receiver. It is assumed that the devices are uniformly distributed over the surface of the Earth. The model requires an estimate of the path gain over the geographical area surrounding the receiver, the average receiver and transmitter antenna gains, and the average areal density of transmitters. The areal path gain can be calculated from traditional propagation models such as the Irregular Terrain Model [2]. A simple methodology that can be used to estimate average transmitter antenna gain is given in this subsection. Example calculations are given using simple receiving and transmitting antennas.

Let a UWB device with EIRP w_t and gain g_t be located at a point in space denoted by λ_i . The gain due to free space and terrestrial propagation from the point λ_i to the victim receiver, g_b , is a random variable that depends on location, terrain, climate, and other factors. Assuming a receiver gain g_r , the received power is

$$w_r = g_r w_t g_t g_b(\lambda_i, \omega_i) \quad , \quad (4.5)$$

where λ_i represents the dependence on the spatial location and ω_i are points in some probability space that characterizes, for example, random variations in devices, how, when and where they are deployed, propagation paths, etc. The average power at the victim receiver due to

many UWB devices is obtained by taking the expected value of the sum of the contribution from each device

$$\begin{aligned}\bar{w}_r &= \mathcal{E} \left\{ \sum_i g_r w_i g_t g_b(\lambda_i, \omega_i) \right\} \\ &= \mathcal{E} \left\{ \sum_{\Delta\lambda} n(\Delta\lambda) g_r w_i g_t g_b(\Delta\lambda, \omega_i) \right\},\end{aligned}\quad (4.6)$$

where $\Delta\lambda$ is an area increment at the point λ_i and $n(\Delta\lambda)$ is the number of devices in $\Delta\lambda$.

In this model, it will be assumed that the devices are randomly distributed in space according to *Poisson Postulates*. Essentially this means that the number of devices in non-overlapping regions of space are *independent*, the probability structure is both space and time invariant, and the probability of exactly one device being in a small increment of space $\Delta\lambda$ is approximately proportional to the increment

$$p(\Delta\lambda) = \rho \Delta\lambda + o(\Delta\lambda); \quad \Delta\lambda \rightarrow 0, \quad (4.7)$$

where ρ is the average density. The probability of more than one device being in a small interval is smaller than the order of magnitude of $\Delta\lambda$ (i.e., $o(\Delta\lambda)$). The average received power is then

$$\bar{w}_r = \rho \sum_{\Delta\lambda} \mathcal{E} \{ w_i g_t g_r g_b(\lambda_i, \omega_i) \} \Delta\lambda. \quad (4.8)$$

The expected values of the transmitted power \bar{w}_t and gain \bar{g}_t will depend, for example, on the range of possible devices and the antenna orientations with respect to the victim receiver. The mean path gain \bar{g}_b is a function of the space coordinates. The mean receiver gain \bar{g}_r will also in general be a function of the space coordinates. Assuming a distribution in 2-space corresponding to the surface of the earth, for small increments, the received power can be calculated via integration. Using polar coordinates with the victim receiver located at the origin, the average power (assuming \bar{g}_r and \bar{g}_b are independent) is

$$\bar{w}_r = \bar{w}_t \bar{g}_t \rho \int_0^{2\pi} \bar{g}_r(\phi) d\phi \int_0^\infty \bar{g}_b(r) r dr. \quad (4.9)$$

In this expression, the basic path gain is the average over all possible radial paths and may be calculated, for example, by using the Irregular Terrain Model in the *area prediction mode*. The integral over ϕ includes the directive gain of a typical receiver. In this model, the parameter ρ is constant and is equal to the average number of devices per unit area.

4.3.1 Example Calculation Using the Irregular Terrain Model (ITM)

Converting Equation 4.9 to decibels, we have

$$\begin{aligned}\bar{W}_r &= \bar{W}_t + \bar{G}_t + P + \Gamma_r + \Gamma_b \\ \Gamma_r &= 10 \log_{10} \frac{1}{2\pi} \int_0^{2\pi} \bar{g}_r(\phi) d\phi \\ \Gamma_b &= 10 \log_{10} 2\pi \int_0^{\infty} \bar{g}_b(r) r dr\end{aligned}\tag{4.10}$$

As is customary, upper case letters are used to denote decibel equivalents. The mean transmitter power can be estimated from specifications or measurements of typical UWB devices.

A Method for Estimating \bar{G}_t

In this model, it is assumed that the transmitting antennas are randomly oriented. The average is obtained by assuming a probability distribution for the orientations and applying a typical UWB transmitter gain function which can be defined in terms of the usual spherical coordinate system angles θ and α . In what follows, θ is the angle from the pole of the sphere located, for example, at the top of the transmitter antenna (e.g., the top of a vertical dipole) and α is the azimuth.

In the case of a victim receiver near the ground, it is reasonable to assume that the direction of propagation to the receiver is uniformly distributed over a solid angle Ω_0 defined by a *band* on the unit sphere bounded by spherical angles θ_0 and $\pi - \theta_0$ ($0 \leq \alpha \leq 2\pi$). The expected value of the gain in the direction of the victim receiver in terms of the directive gain function $g_t = f(\Omega)$ is

$$\mathcal{E}\{f(\Omega)\} = \int_{\Omega_0} f(\Omega) \frac{d\Omega}{\Omega_0},\tag{4.11}$$

where

$$\Omega_0 = 2 \int_0^{2\pi} \int_{\theta_0}^{\pi/2} \sin \theta \, d\theta \, d\alpha = 4\pi \cos \theta_0 \quad (4.12)$$

The expected value of g_r is then

$$\mathcal{E}\{f(\theta, \alpha)\} = \frac{1}{4\pi \cos \theta_0} \int_0^{2\pi} \int_{\theta_0}^{\pi-\theta_0} f(\theta, \alpha) \sin \theta \, d\theta \, d\alpha \quad (4.13)$$

As an example, consider a short dipole where $f(\theta, \alpha) = 1.5 \sin^2 \theta$. The expected value of the gain is

$$\mathcal{E}\{g_r\} = 1.5 \left(1 - \frac{\cos^2 \theta_0}{3} \right) \quad (4.14)$$

When the transmitters are oriented so that $\theta_0 \approx \pi/2$, $\bar{G}_r \approx 1.76$ dB and when $\theta_0 = 0$, $\bar{G}_r = 0$ dB.

Calculation of Areal Gain Γ_b Using ITM

The ITM in area prediction mode was used to obtain the average path gain \bar{g}_p relative to free space g_{fs} as function of distance from the victim receiver. The basic path gain $\bar{g}_b = \bar{g}_p g_{fs}$ was then integrated to obtain Γ_b . Table 4.1 gives typical ITM parameter settings used for examples given below unless otherwise specified.

Referring to Equation 4.10, the basic path gain is integrated over the interval $[0, \infty]$. The usual free space gain formula is only valid in the far field and has a singularity at $r = 0$. In the near field (less than a few wavelengths), power is transferred between the antennas via *mutual* coupling. For the purposes of this analysis, close proximity free space coupling was approximated by fitting a function to data obtained from a numerical analysis of the maximum coupling between two half-wave dipoles in the near field [3]. The resulting function used to calculate free space gain is

$$G_{fs} \approx -20 \log_{10} \left(\frac{4\pi r}{\lambda} + 1.64 \right) \quad , \quad (4.15)$$

which closely approximates near-field results and gives the usual far-field behavior when the antennas are separated by more than a few wavelengths. The numerical results for near-field coupling and G_{fs} (maximum coupling less the gain of the half-wave dipoles) as a function of antenna separation are shown in Figure 4.1.

For large distances, the integration is truncated well into the diffraction region (beyond the smooth earth radio horizon) where contributions are negligible. Figure 4.2 shows the basic transmission gain \bar{G}_b and path gain \bar{G}_p , obtained from ITM for the parameters given in Table 4.1.

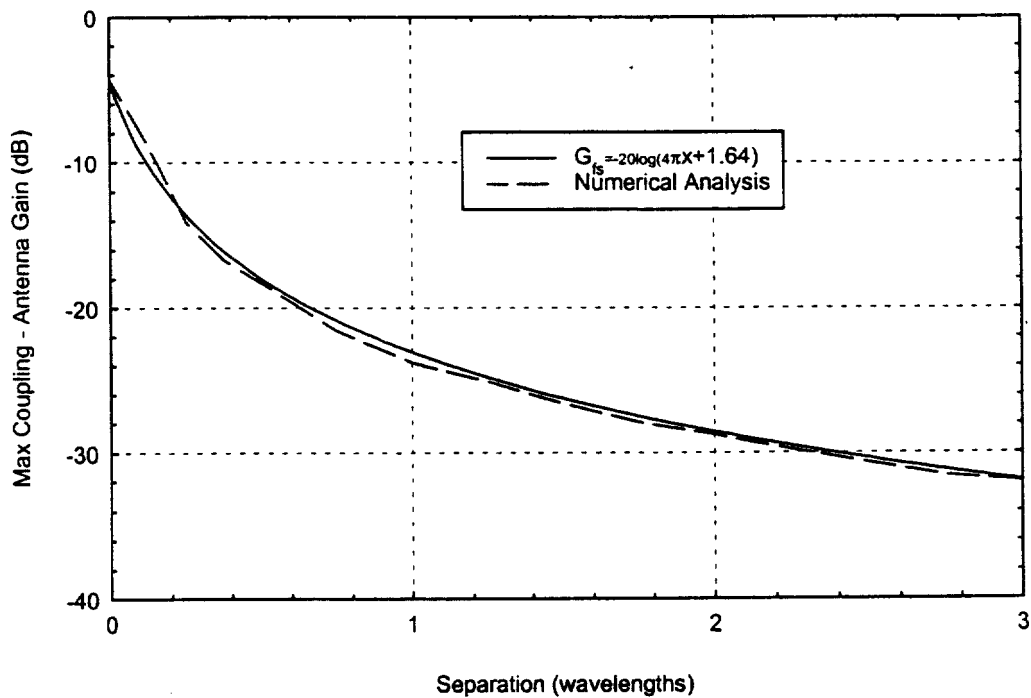


Figure 4.1 Approximation for near field antenna coupling.

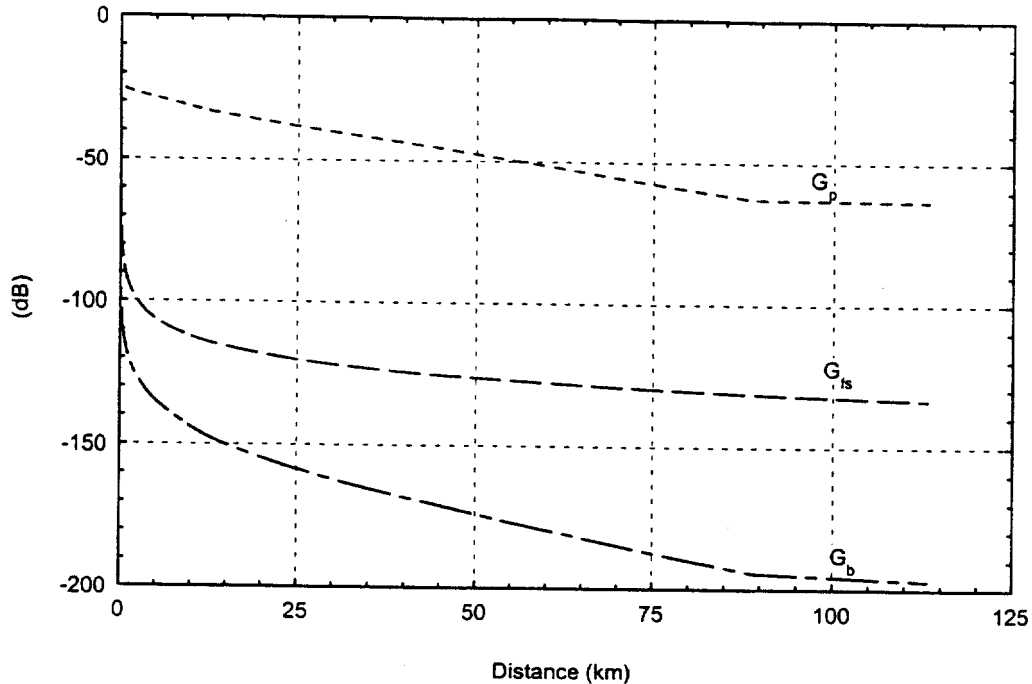


Figure 4.2. Example calculation of basic transmission gain G_b using ITM. G_p is the path gain and G_{fs} is the free-space gain. (1000 MHz, $\Delta h=90$ m, $T_x = 2$ m, $R_x = 3$ m).

Effects of Δh and Receiver Height

In area prediction mode, the statistical parameter Δh is used to characterize terrain in the geographical region of interest. The dependence of the parameter Γ_b on Δh is shown in Figure 4.3. Of note is the fact that in *flat* terrain Γ_b is more than 20 dB greater than for *hilly* terrain ($\Delta h = 90$ m).

In Figure 4.4, the parameter Γ_b is plotted as a function of receiver height. Basically, the path gain increases with increasing antenna height since terrestrial attenuation is not a factor at increasing distances from the receiver (as the receiver height increases). With increasing height, the path gain from the entire region within line-of-sight of the receiver is essentially due to free space propagation.

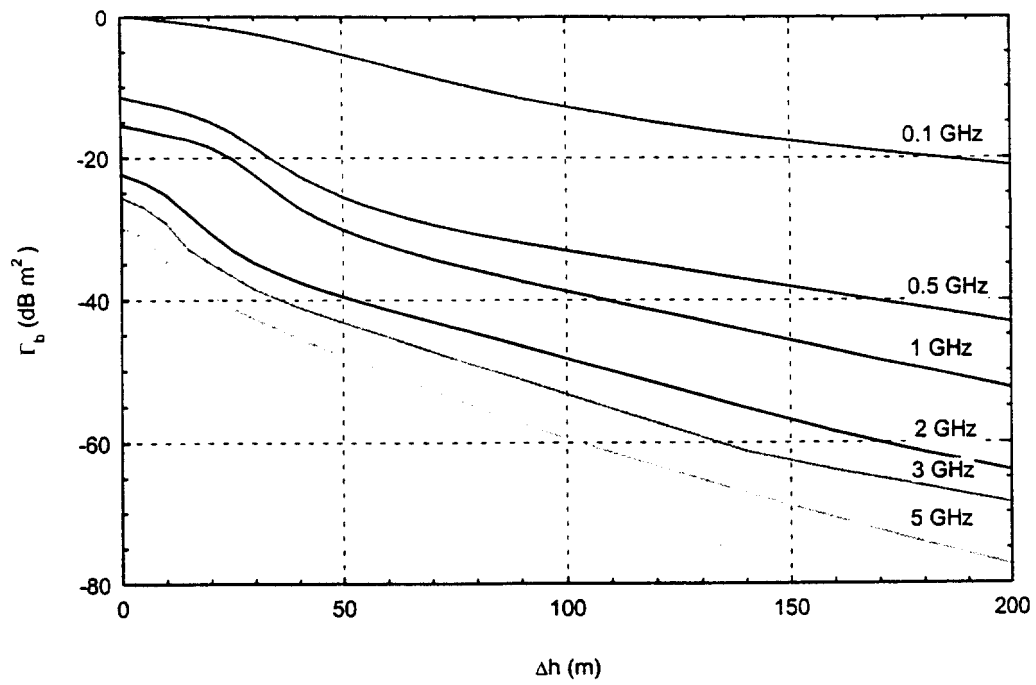


Figure 4.3. Basic areal gain Γ_b as a function of Δh and frequency. ($T_x = 2$ m, $R_x = 3$ m).

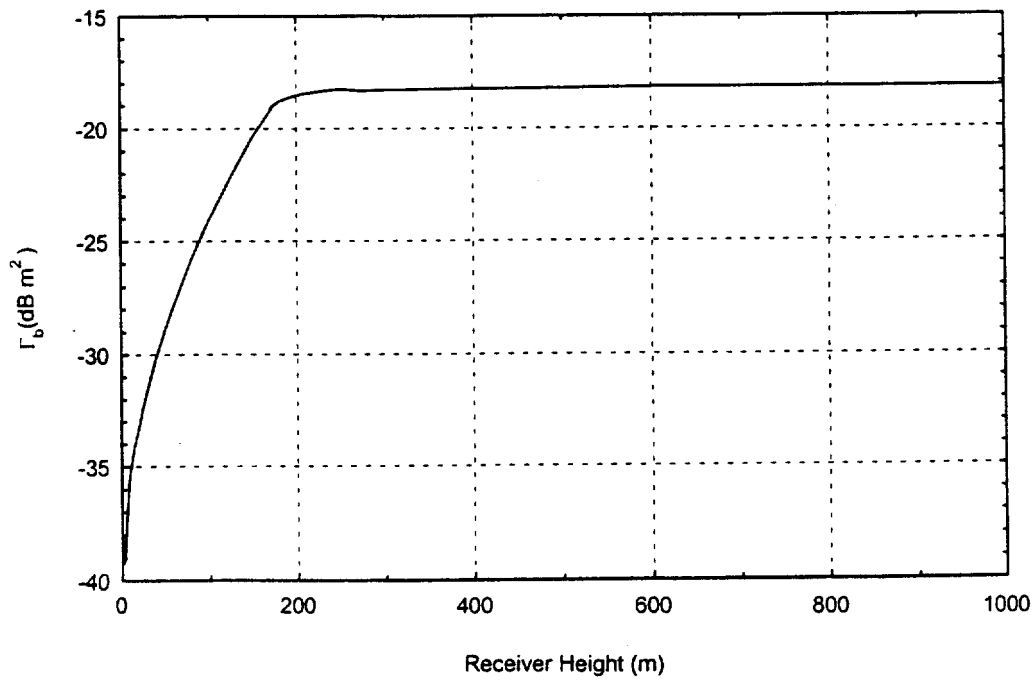


Figure 4.4. Basic areal gain Γ_b as a function of receiver height. (1000 MHz, $\Delta h = 90$ m).

Table 4.1 Parameters for ITM Calculations

ITM Parameter	Value
Frequency	Various
Receiver Antenna Height	3 m
Transmitter Antenna Height	2 m
Polarization	Vertical
Terrain Irregularity Parameter Δh	90 m, 30 m, 0
Ground Electrical Constants	.005 S/m, $\epsilon_r = 15$
Surface Refractivity	301 N-units
Climate	Continental Temperate
Siting Criteria	Random
Time and Location Variability	50%
Confidence	50%

Estimated Interference Power Levels for a Half-wave Dipole Receiver

Referring to Equation 4.9, azimuthal dependence of the receiver gain in the direction of the UWB transmitters can be explicitly included in the analysis. The quantity Γ_r , defined in Equation 4.10 is just the *average* gain in the azimuthal direction. To give a simple example, a half-wave dipole has a constant azimuthal gain of 2.15 dBi, hence $\Gamma_r = 2.15$ dBi.

Assuming that the UWB transmitters are short dipoles and $\bar{G}_t = 1.76$, the power at the receiver per watt of transmitted power is

$$W_r = 3.91 + P + \Gamma_b \text{ dBW} \quad , \quad (4.16)$$

where P is the average density in dB per unit area, and Γ_b is *area average of path gain*. Calculated values for various frequencies and terrain parameters associated with so called *flat* ($\Delta h = 0$), *plains* ($\Delta h = 30$ m), and *hills* ($\Delta h = 90$ m) environments are given in Table 4.2 below.

Table 4.2 Γ_b as a Function of Δh and Frequency (Based on Parameters Given in Table 4.1)

Frequency (MHz)	Γ_b dB m ²		
	$\Delta h = 0$	$\Delta h = 30m$	$\Delta h = 90m$
100	0.14	-2.51	-11.61
500	-11.46	-18.56	-31.97
1000	-16.84	-27.48	-39.11
1500	-20.03	-32.02	-43.35
2000	-22.32	-34.88	-46.53
2500	-24.10	-36.93	-49.13
3000	-25.56	-38.53	-51.26
3500	-26.81	-39.84	-53.11
4000	-27.89	-40.97	-54.74
4500	-28.83	-41.96	-56.24
5000	-29.69	-42.77	-57.51

4.3.2 Example Calculation Assuming Free Space Propagation to the Radio Horizon

When the victim receiver is located high above the earth, as with an aircraft receiver, the transmission path to the radio horizon is largely unaffected by the earth (see Figure 4.4). In such cases, the interfering signal power can be estimated by assuming free space propagation to all devices located within the radio horizon. It should be noted that the methodology described below neglects the effects of line-of-sight propagation in the troposphere and that due to diffraction and tropospheric scatter from beyond the radio horizon. The over-the-horizon diffracted and scattered signals will be minimal in most cases of interest.

The areal gain Γ_b is calculated from

$$\Gamma_b = 10 \log_{10} \frac{\lambda^2}{8\pi} \int_0^{r_{horiz}} \frac{r dr}{(h_r - h_t)^2 + r^2} \quad , \quad (4.17)$$

where h_r is the height of the receiver, h_t is the height of the transmitter, and r_{horiz} is the distance to the radio horizon which can be calculated using the following approximate expression [2]

$$r_{horiz} = \sqrt{2h_r/\gamma_e} + \sqrt{2h_t/\gamma_e} = \sqrt{2a_e h_r} + \sqrt{2a_e h_t} \quad . \quad (4.18)$$

The earth's effective curvature γ_e is the reciprocal of the earth's effective radius a_e and is normally determined from the surface refractivity using the empirical formula [2]

$$\begin{aligned} \gamma_e &= \gamma_a / K \\ a_e &= K a \\ K &= \left(1 - 0.04665 e^{N_s/N_1}\right)^{-1} \quad , \end{aligned} \quad (4.19)$$

where K is the *effective earth radius factor*, N_s is the surface refractivity, $N_1 = 179.3$ N-units, and $\gamma_a = 1/a = 157 \times 10^{-9} \text{ m}^{-1} = 157$ N-units/km [2].

Evaluating the integral in Equation 4.17 gives

$$\Gamma_b = 10 \log_{10} \left(\frac{\lambda^2}{16\pi} \log_e \left(\frac{(h_r - h_t)^2 + r_{horiz}^2}{(h_r - h_t)^2} \right) \right) \quad . \quad (4.20)$$

When the receiver height is much greater than the transmitter height the result can be reduced to

$$\Gamma_b = 32.52 - 20 \log_{10} f_{MHz} + 10 \log_{10} \log_e \left(1 + \frac{2Ka}{h_r} \right) \quad dB \text{ m}^2 \quad . \quad (4.21)$$

Assuming a standard four thirds earth ($K = 4/3$), Figure 4.5 shows the areal gain as a function of frequency and receiver antenna height as compared with Γ_b calculated using the ITM up to its recommended limit of 1 km. Note that at 1 km, the results are within about 0.5 dB. Using Equation 4.21, Figure 4.6 shows Γ_b for various frequencies as a function of receiver height up to 10 km.

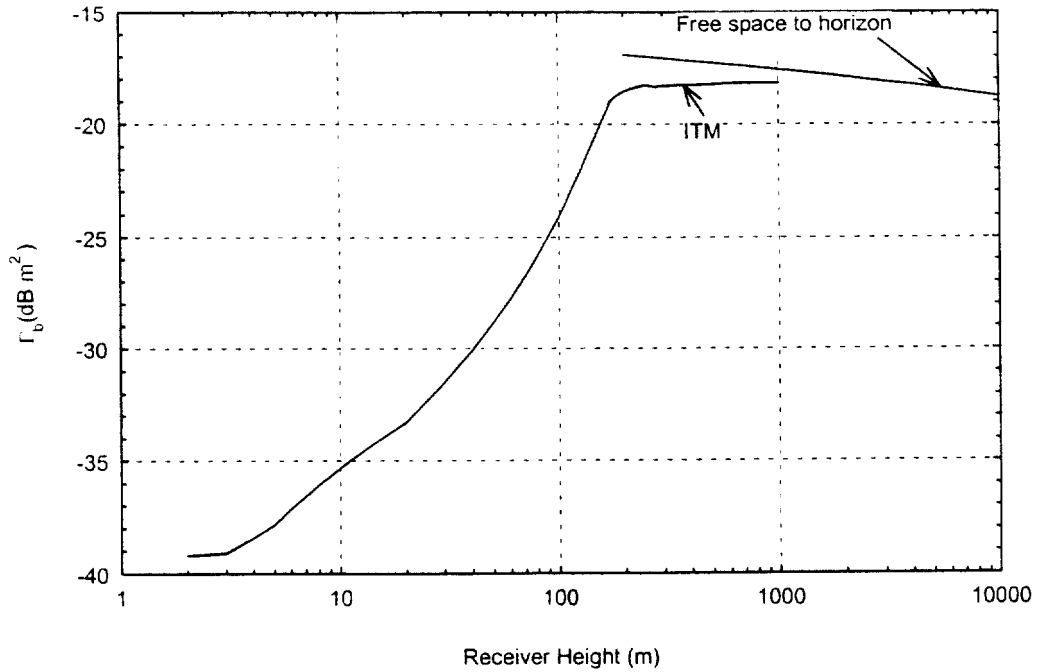


Figure 4.5. Basic areal gain Γ_b as a function of receiver height using ITM compared with a direct calculation assuming free-space propagation. (1000 MHz, $\Delta h=90$ m).

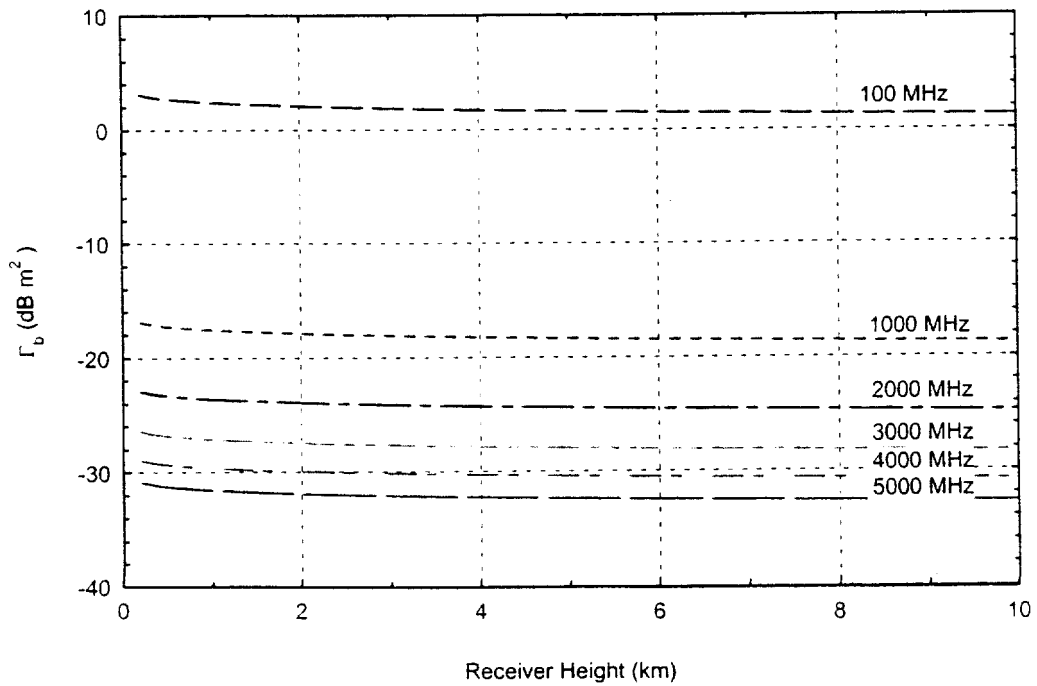


Figure 4.6. Basic areal gain Γ_b as a function of receiver height assuming free-space gain to the radio horizon.

4.4 References

- [1] Harald Cramer, *Mathematical Methods of Statistics*, Princeton NJ: Princeton University Press, 1945.
- [2] G.A. Hufford, A.G. Longely, and W. Kissick "A guide to the use of the ITS irregular terrain model in the area prediction mode," NTIA Report 82-100, April 1982.
- [3] Constantine A. Balains, *Antenna Theory Analysis and Design*, 2nd Edition, New York: John Wiley and Sons, 1997, p 442.

5. FULL-BANDWIDTH REFERENCE MEASUREMENTS OF ULTRAWIDEBAND EMISSIONS

Brent Bedford,¹ Robert T. Johnk,² and David R. Novotny²

5.1 Introduction

Ultrawideband (UWB) signals, by definition, contain energy over a larger range of the frequency spectrum than do conventional radio signals which are relatively narrow-banded. The majority of conventional radio test equipment, however, are designed to measure the signals from the majority of radio systems in use, which constitute mostly narrowband and a few wideband signaling systems. UWB is a new class of signals that places new demands on measurement equipment.

There exists a need to characterize this new class of signals across their full emission bandwidth. This section describes measurements that address that need by capturing the pulse shapes and inner pulse structure from a selection of UWB devices. The UWB signals in this study are very narrow pulses of RF energy that are modulated or envelope-shaped in various ways. This study provides a view of the UWB pulses that cannot be directly measured with common narrower bandwidth equipment. From this full-bandwidth view of the pulses, comparisons can be made with measurement results performed with conventional equipment. The measurement results in this section provide a reference to which other measurement results can be compared, to see how well the reference set of signal parameters can be predicted from measurements using bandwidth-limited equipment.

5.2 Measuring Instruments and Calculation Methods

The signals emitted from a selection of UWB devices (see section 1.2) were measured by the National Institute of Standards and Technology (NIST) Radio-Frequency Technology Division to obtain data that represents the radiated time-domain waveform. The goal of these measurements was to capture a detailed view of a single pulse. The pulses were measured in two different environments. The first environment was called "conducted measurements." The second environment was called "radiated measurements."

¹The author is with the Institute for Telecommunication Sciences, National Telecommunications and Information Administration, U.S. Department of Commerce, Boulder, CO 80305.

²The authors are with the Radio-Frequency Technology Division, National Institute for Standards and Technology, U.S. Department of Commerce, Boulder, CO 80305.

Two different measuring instruments were used in making the full-bandwidth measurements. The first instrument was a sampling oscilloscope. This instrument was capable of achieving very high equivalent sample rates when digitizing the input signal. The instrument used in this study possessed a bandwidth of 20 GHz with the ability to acquire 4,096 samples in a single time-domain record. Due to the nature of how this instrument performs its sampling, it had two limitations. The repetition rate of the pulses to be measured must be constant and the pulse shape invariant. While some UWB devices satisfy this requirement, there are devices that do not and were measured by a second measuring instrument.

The second measuring instrument was a single-event transient digitizer. This instrument had the advantage of placing fewer restrictions on the pulse parameters that it can measure. The digitizer possessed a bandwidth of 4.5 GHz with a maximum of 1,024 samples in a single shot. The instrument was designed to perform high fidelity measurements on a single pulse.

Two quantities were calculated from each measured waveform. The first quantity was "Total Peak Power." Given that there are i sample points in the time-domain waveform and x is the i th sample point, total peak power was calculated using equation 5.1 and was the maximum i th value of the power vector.

$$power_i = \frac{x_i^2}{50} \quad (5.1)$$

The second quantity was "Total Average Power." It was calculated as shown in equation 5.2.

$$Average\ Power = \frac{1}{pri} * \sum_i \left(\frac{x_i^2}{50} \right) * \Delta t \quad (5.2)$$

where x_i is the i th time-domain sample
 Δt is the sample interval
 pri is the pulse repetition interval

The PRI that was used in the calculation is the shortest time interval between any two pulses. Effects which could lengthen the PRI such as On-Off-Keying or the quiet time between bursts of pulses were not considered since measuring these parameters was beyond the scope of this investigation. Some devices could operate with more than one mode setting. For these devices, the maximum and minimum PRIs were used in the calculation.

5.3 Conducted Measurements

Two different test setups were implemented for the conducted measurements. The first is shown in Figure 5.1. The RF output of the UWB device-under-test was connected using a coaxial transmission line to an attenuator. The attenuator was used to prevent overloading and damage to the measurement instrument from too strong a signal level. The signal was then split into two equal amplitude levels and fed into a trigger port and a signal port on a sampling oscilloscope. Several pulses were measured to check for pulse shape variations that might induce measurement errors. This setup was used to perform conducted measurements on device A, which has a constant pulse repetition frequency.

The second test setup is shown in Figure 5.2. The only difference from Figure 5.1 is the use of a single-event transient digitizer. This setup was used to perform conducted measurements on devices B and D due to a non-constant pulse repetition rate in the emissions.

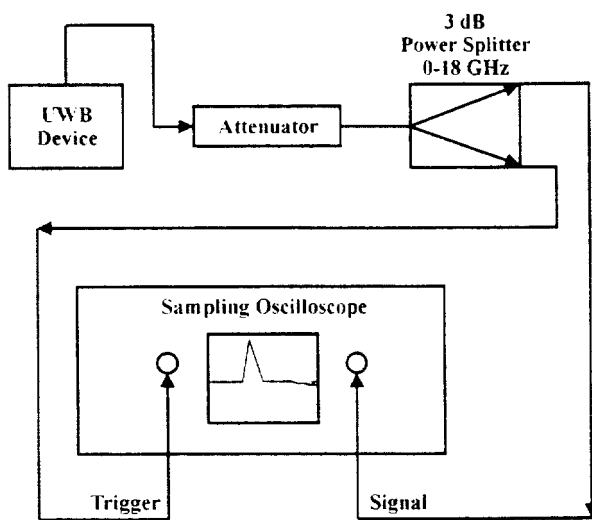


Figure 5.1. Device A, conducted measurement test setup.

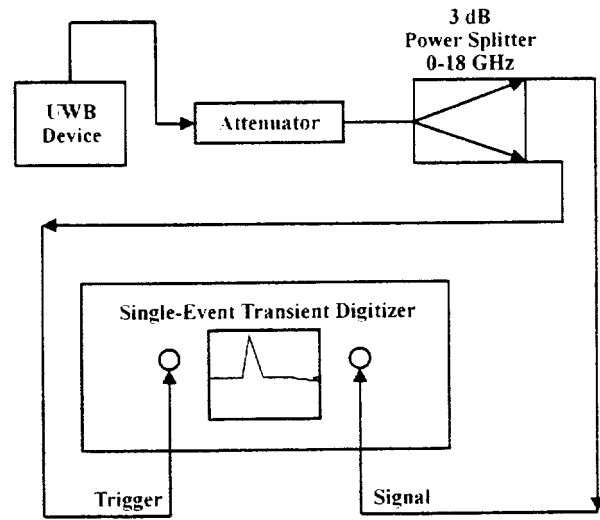


Figure 5.2. Device B and D, conducted measurement test setup.

The measured time-domain waveform for device A is shown in Figure 5.3. It exhibits a large main pulse followed by some damped ringing. The vertical axis represents voltage at the RF output connector of the UWB device. The corresponding frequency-domain power spectrum, which was calculated from the time-domain waveform, is shown in Figure 5.4. The vertical axis represents decibels relative to a milliwatt at the RF output connector of the UWB device. The caption presents a Δf number which is the frequency spacing between the graphed points.

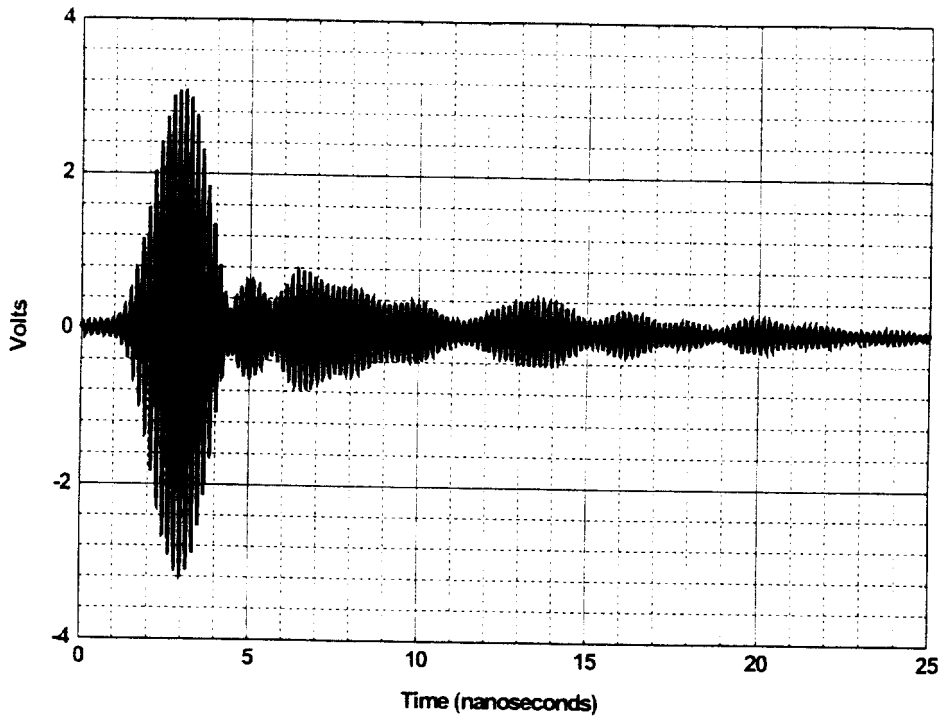


Figure 5.3. Device A, conducted time-domain waveform.

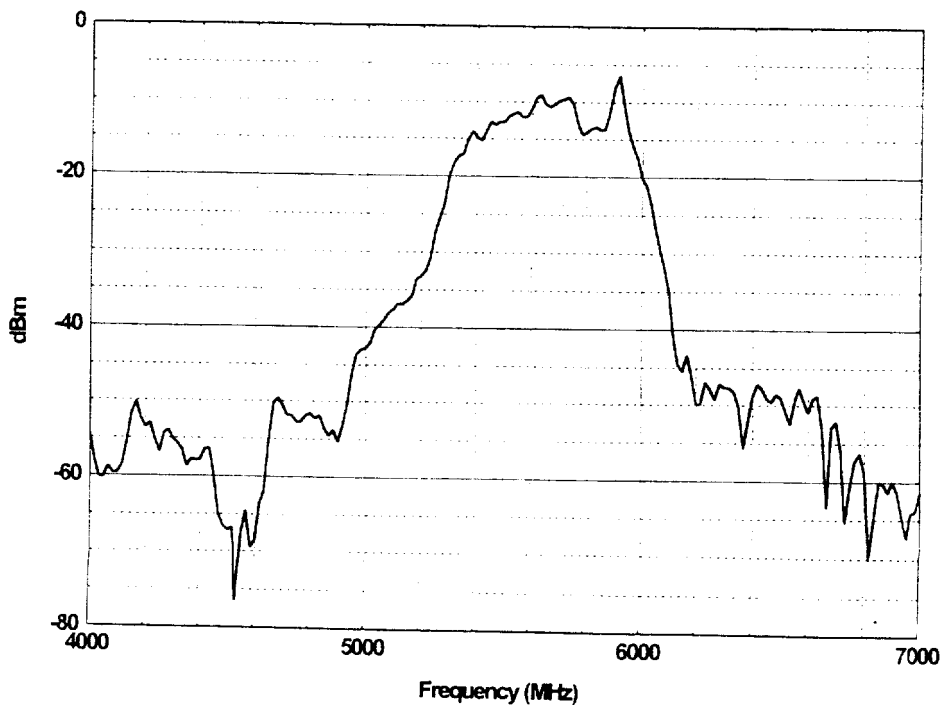


Figure 5.4. Device A, conducted power spectrum. $\Delta f = 16.67$ MHz.

The following table summarizes the Total Peak Power and the Total Average Power calculated for the devices for which conducted measurements were performed.

Table 5.1. Total Peak and Total Average Powers from the Conducted Measurements.

Device Letter	Total Peak Power (dBm)	Total Average Power (dBm)
A	23.1	-27.8
B	32.0	-4.5
D	17.4	-16.0

The -10 and -20 dB bandwidths were extracted from the frequency-domain power spectrum graphs. These bandwidths, from the conducted measurements, are summarized below.

Table 5.2. Emission Bandwidth from the Conducted Measurements.

Device Letter	-10 dB Bandwidth (MHz)	-20 dB Bandwidth (MHz)
A	616.6	799.9
B	479.9	539.9
D	1349	2597

Appendix D contains the complete set of conducted measurement graphs for devices A, B, and D.

5.4 Radiated Measurements

Four different test setups were implemented for the radiated measurements. All of the test setups were performed in the NIST anechoic chamber. The first test setup is shown in Figure 5.5. The UWB device-under-test radiates using its manufacturer supplied antenna into the chamber. A ridged horn antenna was used in this configuration. The measurement frequency range using this antenna was 1 GHz to 4 GHz. Two stages of amplification were needed in this configuration to provide enough signal to drive the measuring instrument. A calibration was performed on the amplifiers to provide a frequency response correction. The signal was then split into two equal amplitude levels and fed into a trigger port and a signal port on a single-event transient digitizer. This setup was used to perform radiated measurements on device C. Figure 5.6 shows the second test setup that was used. The only difference from the previous test setup is a single stage of amplification since this UWB device produced a stronger signal. This setup was used to perform radiated measurements on device D. Figure 5.7 shows the third setup. The only difference from the previous test setup is the use of a different receiving antenna. The receiving antenna was a NIST 30 cm TEM horn, which produces minimal waveform distortion. The measurement

frequency range using this antenna was 200 MHz to 4000 MHz. This setup was used to perform radiated measurements on device E (1500 MHz and 900 MHz modes). Figure 5.8 shows the fourth test setup. The only difference from the previous test setup is the addition of an attenuator to trim the measurement system gain down to an optimum level for the measurement. The NIST 30 cm TEM horn was used in this measurement as the receiving antenna. This setup was used to perform radiated measurements on device E (300 MHz mode) and B.

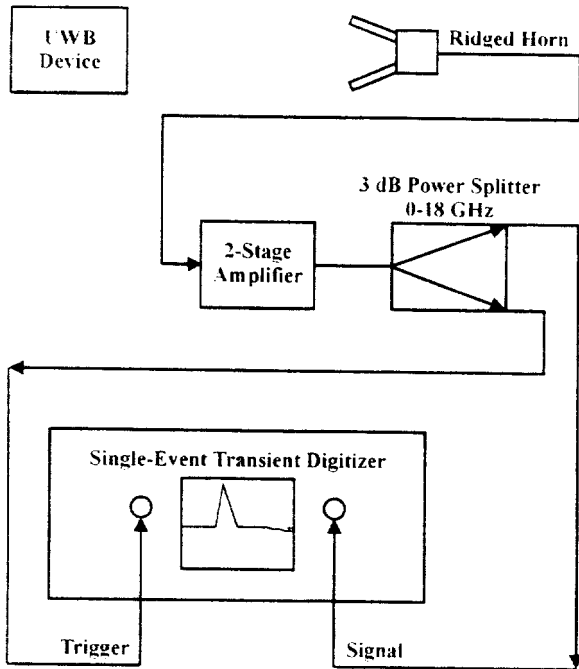


Figure 5.5. Device C, radiated measurement test setup.

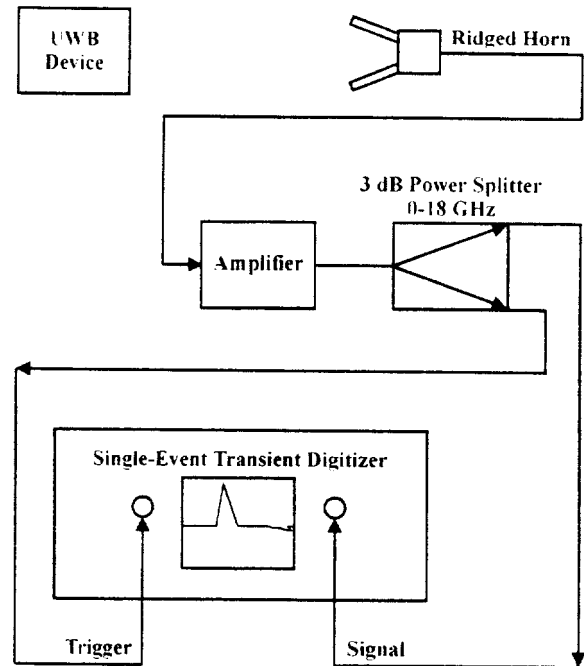


Figure 5.6. Device D, radiated measurement test setup.

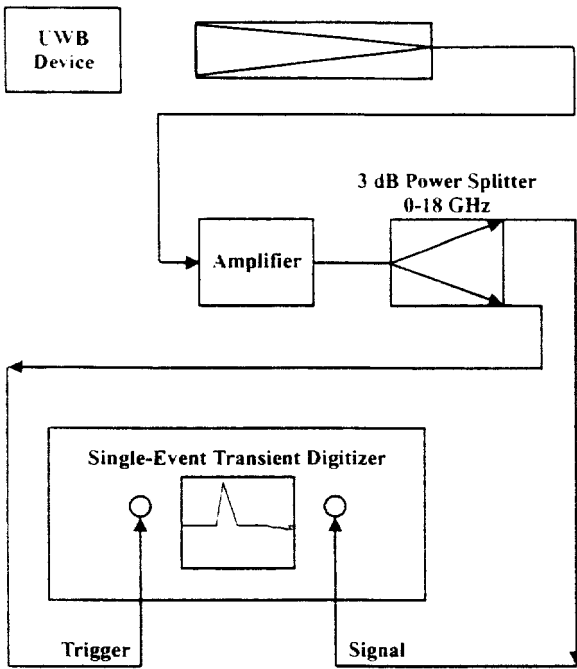


Figure 5.7. Device E (1500 MHz and 900 MHz), radiated measurement test setup.

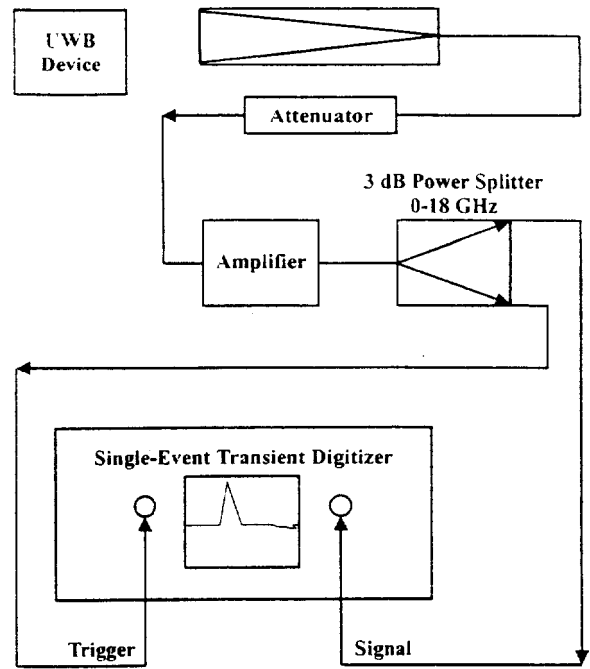


Figure 5.8. Device E (300 MHz) and B, radiated measurement test setup.

The measured time-domain waveform for device C is shown in Figure 5.9. The vertical axis represents voltage at the receiving antenna terminals. The separation distance between the receiving antenna and the transmitting antenna was one meter. The corresponding frequency-domain spectrum is shown in Figure 5.10. The vertical axis represents field strength (decibels relative to a microvolt per meter), calculated from the time-domain waveform, at the receiving antenna's location. The caption presents a Δf number, which is the frequency spacing between the graphed points.

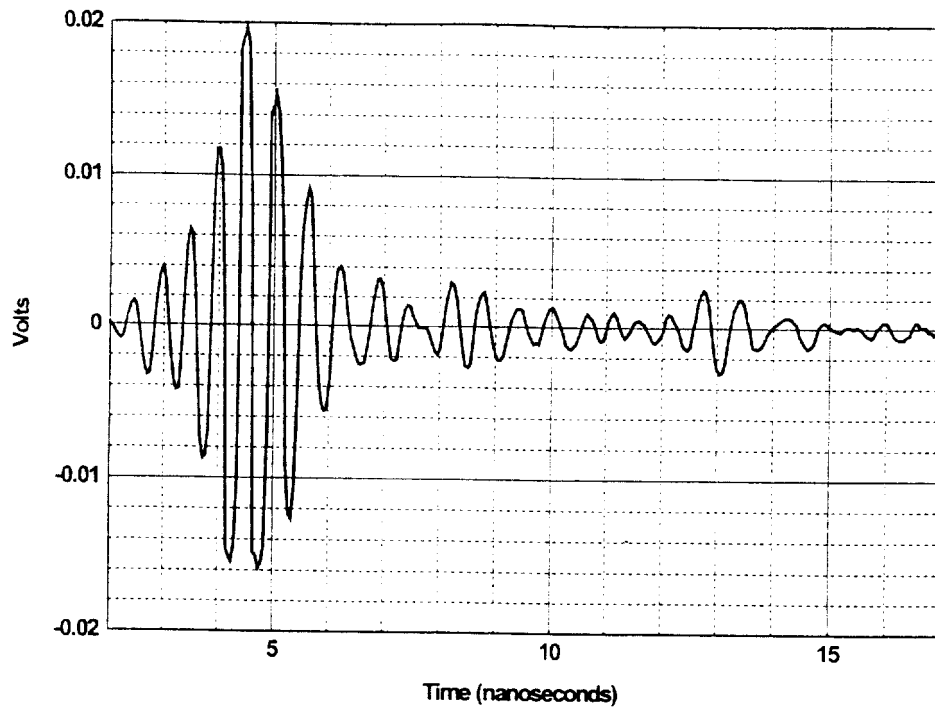


Figure 5.9. Device C, radiated time-domain waveform.

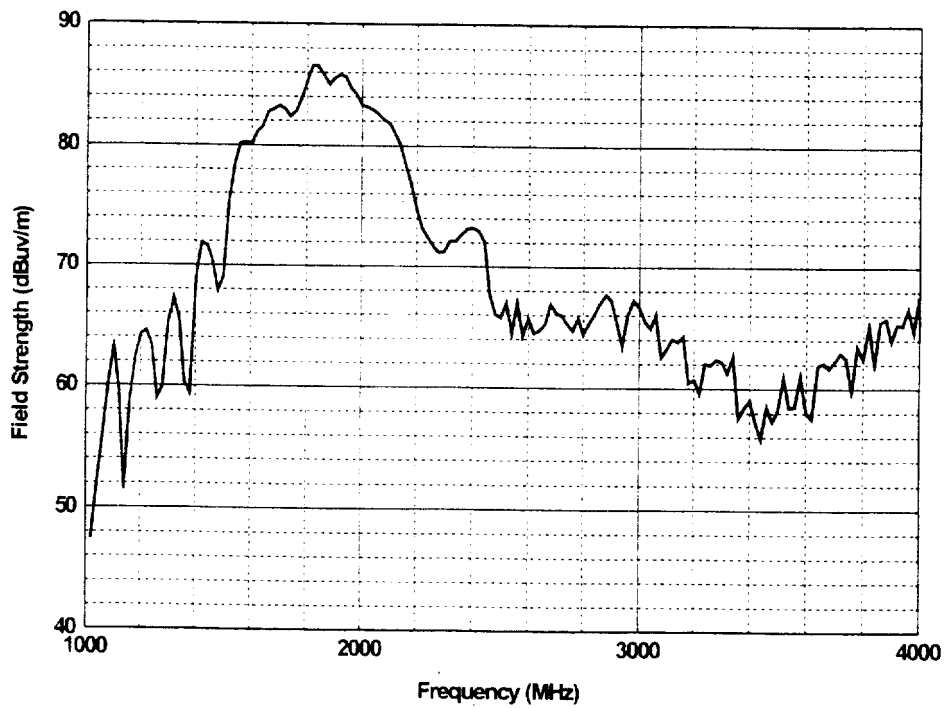


Figure 5.10. Device C, radiated peak field strength at 1 m, $\Delta f = 20$ MHz.

The following table summarizes the Total Peak Power and the Total Average Power calculated for the devices for which radiated measurements were performed.

Table 5.3. Total Peak and Total Average Powers from the Radiated Measurements.

Device Letter	Total Peak Power (dBm)	Total Average Power (dBm)
B (maximum PRI)	-3.2	-39.8
B (minimum PRI)	-3.2	-33.7
C	-21.1	-48.6
D (maximum PRI)	-20.5	-51.8
D (minimum PRI)	-20.5	-41.8
E (1500 MHz)	-7.9	-55.6
E (900 MHz)	-3.7	PRI unknown
E (300 MHz)	12.5	PRI unknown

The -10 and -20 dB bandwidths were extracted from the frequency-domain radiated spectrum graphs. Some of the devices had combinations of center frequency and bandwidth such that the portion of the spectrum of interest exceeded the valid frequency range of the radiated measurements. The bandwidth could not be determined so these cases are marked with "NA". The bandwidths, from the radiated measurements, are summarized below.

Table 5.4. Emission Bandwidths from the Radiated Measurements .

Device Letter	-10 dB Bandwidth (MHz)	-20 dB Bandwidth (MHz)
B	319.9	539.9
C	659.8	1080
D	NA	NA
E (1500 MHz)	2799	NA
E (900 MHz)	1650	NA
E (300 MHz)	NA	NA

Appendix D contains the complete set of radiated measurement graphs for devices B, C, D, and E. It is interesting to compare the conducted and radiated results for devices B and D. For both devices, the radiated and conducted waveforms are significantly different. While device B's conducted and radiated spectrums look similar, device D's conducted and radiated spectrums are significantly different over the 1 GHz to 2 GHz regions.